Chinese Journal of Aeronautics, (2017), 30(2): 586–594

Chinese Society of Aeronautics and Astronautics
& Beihang University

Chinese Journal of Aeronautics

cja@buaa.edu.cn
www.sciencedirect.com

Experimental study of curvature effects on jet impingement heat transfer on concave surfaces

Zhou Ying [a], Lin Guiping [a], Bu Xueqin [a,*], Bai Lizhan [a,b], Wen Dongsheng [a,b]

[a] *School of Aeronautic Science and Engineering, Beihang University, Beijing 100191, China*
[b] *School of Chemical and Process Engineering, University of Leeds, Leeds LS2 9JT, UK*

Received 27 June 2016; revised 20 October 2016; accepted 21 December 2016
Available online 21 February 2017

KEYWORDS

Anti-icing system;
Concave surface;
Curvature effect;
Heat transfer;
Jet impingement

Abstract Experimental study of the local and average heat transfer characteristics of a single round jet impinging on the concave surfaces was conducted in this work to gain in-depth knowledge of the curvature effects. The experiments were conducted by employing a piccolo tube with one single jet hole over a wide range of parameters: jet Reynolds number from 27000 to 130000, relative nozzle to surface distance from 3.3 to 30, and relative surface curvature from 0.005 to 0.030. Experimental results indicate that the surface curvature has opposite effects on heat transfer characteristics. On one hand, an increase of relative nozzle to surface distance (increasing jet diameter in fact) enhances the average heat transfer around the surface for the same curved surface. On the other hand, the average Nusselt number decreases as relative nozzle to surface distance increases for a fixed jet diameter. Finally, experimental data-based correlations of the average Nusselt number over the curved surface were obtained with consideration of surface curvature effect. This work contributes to a better understanding of the curvature effects on heat transfer of a round jet impingement on concave surfaces, which is of high importance to the design of the aircraft anti-icing system.

© 2017 Chinese Society of Aeronautics and Astronautics. Production and hosting by Elsevier Ltd. This is an open access article under the CC BY-NC-ND license (http://creativecommons.org/licenses/by-nc-nd/4.0/).

1. Introduction

Heat transfer associated with jet impingement on a flat or curved surface has been the subject of extensive investigation for decades because of its enhanced local heat exchange performance in a wide variety of applications such as glass tempering, metal annealing, and engine and turbine blades cooling.[1,2] Impinging jets are also used in the hot-air anti-icing system of commercial aircraft where high-pressure hot air, bleeding from the engine, is ducted forward to a pipe with several small holes on it and impinges on the inner surface of the anti-icing cavity to heat the leading edge of wing. Since the anti-icing cavity is a curved surface, the effect of surface curvature should be taken into account when the jet impingement heat transfer performance is considered.

* Corresponding author.
E-mail address: buxueqin@buaa.edu.cn (X. Bu).

Peer review under responsibility of Editorial Committee of CJA.

http://dx.doi.org/10.1016/j.cja.2016.12.032
1000-9361 © 2017 Chinese Society of Aeronautics and Astronautics. Production and hosting by Elsevier Ltd.
This is an open access article under the CC BY-NC-ND license (http://creativecommons.org/licenses/by-nc-nd/4.0/).

Many experiments were designed to study the heat transfer of impingement jets, with a focus on flat plates. The very early experimental work for the flat plate case were represented by Gardon[3], Goldstein[4], Hrycak[5] and Beltaos et al.[6] with varying impingement distance, Reynolds number and oblique angle. Many measurement techniques based on naphthalene sublimation technique[7], temperature-sensitive liquid crystal[8,9] and thermal infrared camera[10,11] were adopted to measure and analyze the flow and heat transfer characteristics.

Metzger et al.[12] were probably the first to experimentally investigate the heat transfer characteristics of jets impinging on a concave cylindrical surface. The average heat transfer coefficient of single lines of circular jets was obtained with varied ratios of nozzle to surface distance H and nozzle diameter d at the Reynolds range from 1150 to 5500. Results indicated that the maximum heat transfer could be obtained at the optimum relative nozzle to surface $H/d = 3$–5, whose value decreased with increasing Reynolds number. Compared with the heat transfer performance on a flat plate, the stagnation point Nusselt number was higher on the concave cylindrical surface as reported by Hrycak.[13] Mayle et al.[14] also presented that the heat transferred to the boundary layer on the concave plate was greater than that on a flat plate.

Flow visualization facilities with smoke generation wire were applied by Gau and Chung[15] and Cornaro et al.[16] to visualize the flow structure of slot and round jet impinging on concave surfaces. The former result showed that the Nusselt number increased with increasing surface curvature for slot jet impingement on a concave surface, which was caused by the initiation of Taylor-Görtler vortices along the surface. Similar observation was also obtained by Cornaro et al.[16], who also found that the heat transfer rate on and around the stagnation point increased with increasing surface curvature. Lee et al.[17] experimentally investigated the local heat transfer from a long round jet impinging on a smaller relative curvature surface ($d/D = 0.034$, 0.056, 0.089) with jet Reynolds number from 11000 to 50000. Similarly Yang et al.[18] investigated the concave effect but using a slot jet in the range $5920 \leq Re_j \leq 25500$, with a fixed slot-width to diameter ratio of 0.033. Their conclusions were consistent and indicated that the surface curvature and generation of Taylor-Görtler vortices were able to thin the boundary layer and enhance the heat transfer rates further in the downstream region apart from the stagnation point.

Since last decade, impinging jets have been applied to hot-air anti-icing system of aircraft and much progress has been achieved. Brown et al.[19] experimentally investigated the heat transfer in an aircraft nacelle anti-icing system and a correlation of average Nusselt number on the impingement area was presented with consideration of the distance between the jet holes and the jet Reynolds number. Papadakis et al.[20,21] conducted experiments in the NASA Glenn Icing Research Tunnel for a range of external conditions representative of inflight icing. The effects of hot air mass flow and temperature, angle of attack, tunnel airspeed and piccolo jet circumferential placement were investigated. Imbriale et al.[22] used IR thermography to measure 3D surface heat transfer coefficients by a row of jets impinging on a concave surface, representing an airfoil leading edge, and the influences of jet inclination, jet pitch and Reynolds number were analyzed. A more recent study by Bu et al.[23] investigated the heat transfer characteristics of jet impingement on a variable-curvature concave surface of a wing's leading edge experimentally. Parameters including jet Reynolds number, relative nozzle-to-surface distance and jet circumferential placement were considered for the effects on local Nusselt number distributions.

All of above researches indicated an enhanced heat transfer performance of jet impingement on concave surfaces. However the confinement effect of concave surface, which could decrease the heat transfer effect, was seldom studied. When studying 3D temperature distribution of a concave semi-cylindrical surface impinged by round jets, Fenot[24] noticed that the confinement effect actually reduced heat transfer as the average Nusselt number for the flat plate was higher than that for the curved plate. It was believed that the confinement prevented ambient air from mixing with the jet air, and thereby increased the flow temperature. The range of Reynolds number was from 10000 to 23000, and the relative surface curvature $d/D = 0.10$, 0.15, 0.20 and $H/d = 2$–5.

Öztekin et al.[25] investigated the heat transfer characteristics of slot jet impingement on concave surface for jet Reynolds number from 3423 to 9485 and the dimensionless surface curvature $R/L = 0.50$, 0.75 and 1.30, where R was the surface radius and L the surface trace length. Results indicated that, compared with the flat plate, the average Nusselt number along the concave surface was larger when $R/L = 0.75$ and 1.30. The average Nusselt number increased with increasing dimensionless surface curvature R/L, in other words, with decreasing relative surface curvature d/D. A slight increase in Nusslet number with decreasing d/D was also observed in Martin and wright's experiment[26] with single row of round jets impingement on a cylindrical surface. This trend was more prevalent for larger nozzle to surface distances in the range of jet Reynolds number from 5000 to 20000, relative nozzle to nozzle spacing from 2 to 8, nozzle to surface distance from 2 to 8, and $d/D = 0.18$, 0.28.

As briefly reviewed above, although different studies have shown that surface curvature enhanced the heat transfer, detailed mechanism of heat transfer decay on a concave surface is still not well understood. This work conducted an extensive experimental study focusing on the curvature effect along the curved surface. By analyzing the stagnation point Nusselt number, and the average and local Nusselt number distributions in chordwise and spanwise directions, both the enhancement and confinement effects of the surface curvature were investigated. In addition, experimental data-based correlations of the average Nusselt number over the curved surface with consideration of the surface curvature effect were presented and experimentally verified.

2. Experimental apparatus

Fig. 1 schematically shows the jet impinging system used in this investigation. The main elements of the experimental apparatus were a steel pipe with a round nozzle on it and an impingement surface. Both were mounted on independent brackets to keep the surface horizontal and the pipe vertically removable for different nozzle to surface distances. As indicated in Fig. 1, the high pressure air from the air compressor became much cleaner and more stable after passing through the filter and air tank, and then went through the electronic pressure regulator where its pressure was adjusted to the desired value. The adjusted air flowed into the pipe from one

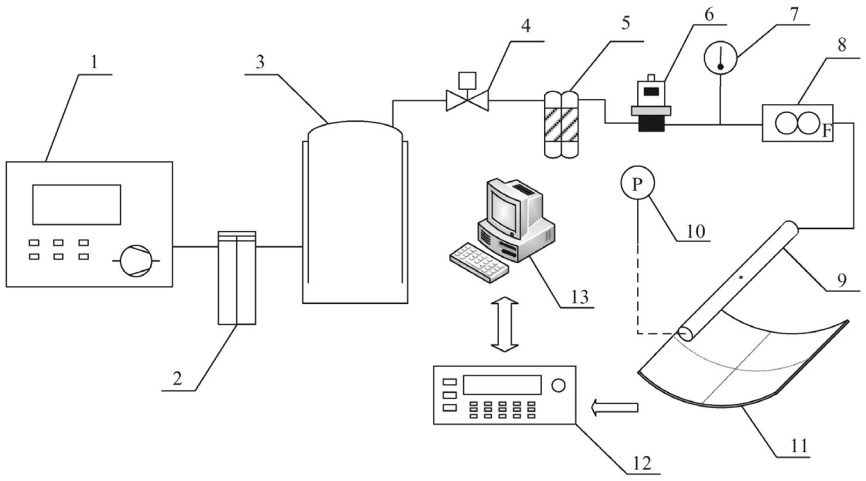

1—Air compressor; 2—Filter; 3—Air tank; 4—Switch valve; 5—Fine filter; 6—Electronic pressure regulator; 7—Temperature sensor; 8—Mass flowmeter; 9—Pipe; 10—Pressure sensor; 11—Impingement surface; 12—Data acquisition instrument; 13—Computer

Fig. 1 Schematic of experimental apparatus.

side and injected into the center of the surface normally through the nozzle. The other side of the pipe was sealed and the pressure inside the pipe was measured by a pressure sensor. The mass flow through the nozzle was measured by a mass flowmeter. The steel pipe had an outer diameter of 20 mm with an inner diameter of 16 mm. Nozzles with diameters d = 1, 2, 3 mm were used with the nozzle to surface distance H = 10, 20, 30 mm, respectively.

The impingement surfaces with different diameters of D = 100 mm, D = 200 mm and a flat surface (regarded as $D = \infty$) manufactured from aluminum plates with a thickness of 2 mm were used in the experiments (Fig. 2). All of these surfaces are kept square with a constant length of L = 150 mm. The relative curvatures can be calculated in Fenot's way[24]: $Cr = d/D$ = 0.005–0.030, or in Öztekin's way[25]: D/L = 0.67, 1.33.

A thin film (0.02 mm thickness) electrical heater made of constantan provided a uniform heat flux on the opposite side of the jet impingement side of the plate. The high pressure jet impinges on the impingement surface as the coolant. This film was engraved as an electronic circuit with equidistant (2 mm width) constantan wires (Fig. 3). Both ends of the film were connected to a DC power supply. In order to reduce the heat loss through the constantan film heater to the ambience, the rubber sponge which has high thermal resistance was

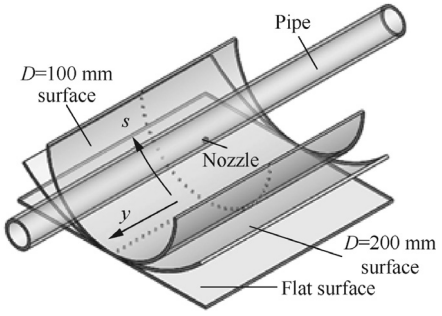

Fig. 2 Test section and impingement plates.

Fig. 3 Constantan film heater.

employed to cover the film heater so that most of the heat would be conducted to the impingement surface, and the small heat loss was corrected in the preliminary test, as described subsequently.

57 type T thermocouples placement was indicated in Fig. 2. The distance between two adjacent thermocouples was constant in both chordwise and spanwise directions. All thermocouple junctions were located in the blind holes on the aluminum plate with a distance of 0.5 mm away from the jet impingement surface and glued by the adhesives of good heat conduction and electrical insulation. The inlet temperature of the pipe and the environment temperature were also measured in the experiment. All the temperature data were acquired by three Agilent 34970A modules and stored in the computer. All the thermocouples were calibrated in the range of 20 °C to 80 °C before the experiment.

3. Data processing

The general definition of Reynolds number is

$$Re = \frac{ud}{v} \tag{1}$$

where v is the kinematic viscosity of air, u the air velocity which is proportional to the jet flow rate and inverse to the sectional area.

Thus, the jet Reynolds number can be defined as

$$Re_j = \frac{\frac{G_m}{\rho\pi(d/2)^2}d}{v} = \frac{4G_m \times d}{\rho\pi d^2\left(\frac{\mu}{\rho}\right)} = \frac{4G_m}{\pi d\mu} \tag{2}$$

where G_m is the jet flow rate, ρ the air density and μ the dynamic viscosity of air.

The heater power Q of the constantan film is accurately determined by measuring both the voltage drop U across and current I through the film.

$$Q = UI \tag{3}$$

The heat flux q in the heated area A is calculated as

$$q = UI/A \tag{4}$$

The local heat transfer coefficient h is defined in terms of the real convective heat flux and the difference between the surface temperature T_s and an appropriate reference temperature T_{ref}. The jet inlet total temperature is employed as the reference temperature in the present experiment.

$$h = \frac{q - q_{loss}}{T_s - T_{ref}} \tag{5}$$

where q_{loss} is the total heat loss caused by radiation and conduction.

The average heat transfer coefficient is calculated from local heat transfer coefficient by area-weighted integral along lines of chordwise (s) and spanwise (y) directions respectively:

$$h_{avg} = \frac{1}{A}\iint h(s,y)\mathrm{d}s\mathrm{d}y \tag{6}$$

The local and average Nusselt numbers can be obtained as follows:

$$Nu = \frac{hd}{\lambda} \tag{7}$$

$$Nu_{avg} = \frac{h_{avg}d}{\lambda} \tag{8}$$

where λ is the thermal conductivity of air.

Table 1 presents the measurement uncertainties of the directly measured parameters, such as the temperature, pressure, voltage and flow rate. Based on the data in Table 1, the uncertainties of h and Nu were all smaller than 4.3%.

Table 1 Uncertainties of measuring equipment.

Equipment	Error
T type thermocouple	±0.4%|T| or 0.3 °C
Pressure transmitter	±0.2% F.S
0–24 V DC power supply	±0.2% F.S
Air mass flow meter	±0.2% F.S

4. Experimental results and discussions

4.1. Preliminary test

Preliminary tests were conducted to calibrate the heat loss and to minimize the experimental error. In the preliminary work, the plate was heated without cold jet impinging on the surface and the temperature data were recorded when the plate came to thermal equilibrium at a certain power applied to the heater. The total heat input is believed equal to the total heat loss caused by radiation and conduction. The total heat loss as a function of temperature difference ΔT between the surface and environment is shown in Fig. 4.

It is indicated from Fig. 4 that the linear correlativity between total heat loss and temperature difference is prominent. The dashed lines are linearly fit for the present experimental results of different plates as described in the following equations:

For flat plate:

$$q_{loss} = 13.354\Delta T, \quad R^2 = 0.9998$$

For D = 200 mm plate:

$$q_{loss} = 14.585\Delta T, \quad R^2 = 0.9974$$

For D = 100 mm plate:

$$q_{loss} = 14.072\Delta T, \quad R^2 = 0.9967$$

where R^2 is the coefficient of determination.

Thus, the corrected heat flux of the impingement surface can be deduced by subtracting the heat loss from the input total heat flux. All the results in this paper are corrected in the same way.

4.2. Effect of jet Reynolds number on Nusselt number

Fig. 5 shows the influence of the jet Reynolds number on the Nusselt number at the stagnation point Nu_{stag} for two concave surfaces at a fixed relative nozzle to surface distance H/d = 10. As shown in Fig. 5, the stagnation point Nusselt number Nu_{stag} increases with jet Reynolds number Re_j for both surfaces. It is mainly because the jet with larger Reynolds number brings more momentum and energy impinging on the stagnation

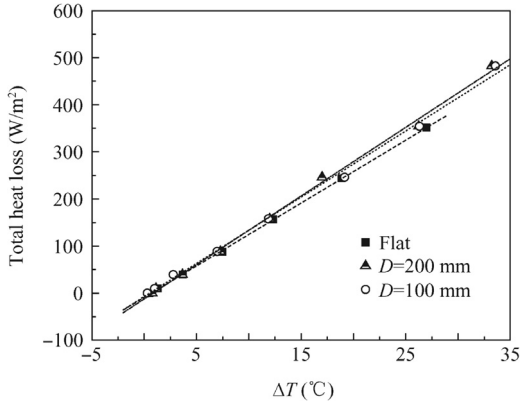

Fig. 4 Total heat loss vs temperature difference between surface and environment.

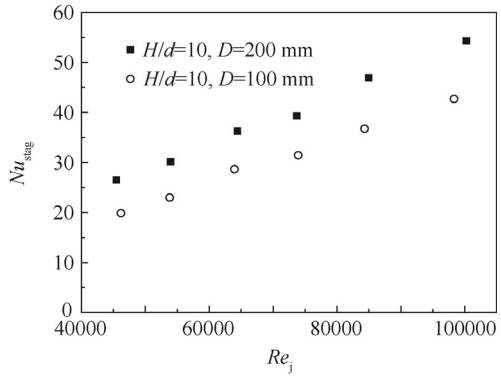

Fig. 5 Influence of jet Reynolds number on Nu_{stag} for $H/d = 10$.

point. Similar results were also shown by other researchers such as Yang et al.[18] and Lee et al.[17] However, in the wall jet region, high Reynolds number offers high velocity and turbulence intensity as a contribution of the generation of Taylor-Görtler vortices, and thus enhances the heat transfer along the streamwise direction, which extends over the entire surface. Therefore, the average Nusselt number Nu_{avg} over the whole surface also increases with increasing Reynolds number (Fig. 6). In brief, the Reynolds number has a significant influence on heat transfer performance at both stagnation point and the entire impingement surface.

4.3. Effect of relative nozzle to surface distance on Nu_s

Fig. 7 shows the distributions of local Nusselt number Nu_s for flat and curved plates with different jet Reynolds numbers in the chordwise direction. Fig. 8 shows the Nusselt number at the stagnation point Nu_{stag} for varying relative nozzle to surface distance H/d. As shown in Fig. 7, the local Nusselt distributions of concave and flat plate indicate the same variation. The effect of H/d on heat transfer is mainly presented near the stagnation region of $s/d < 12.5$, whereas at $s/d > 12.5$, little difference in Nusslet number can be observed. The maximum value in heat transfer distribution occurs at the stagnation point, and the stagnation point Nusselt number declines with increasing H/d (Fig. 8). It is believed that the surrounding air entrained by the high speed jet before impinging on the surface would slow the arrival velocity at the stagnation point. Thus Nu_{stag} decreases with increasing H/d. In addition,

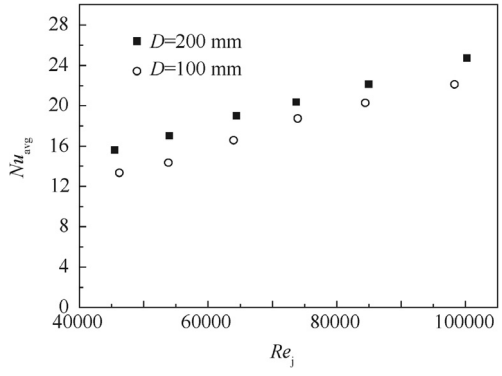

Fig. 6 Influence of jet Reynolds number on Nu_{avg}.

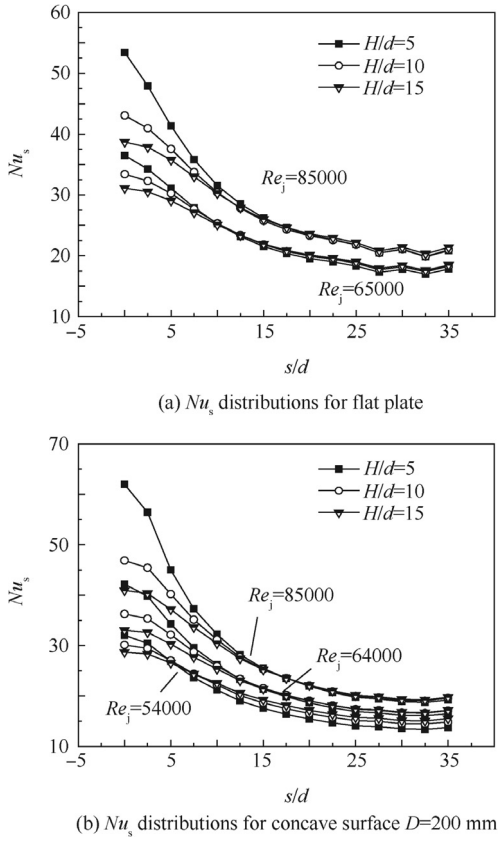

Fig. 7 Local Nusselt number distributions for flat and curved plates in chordwise direction.

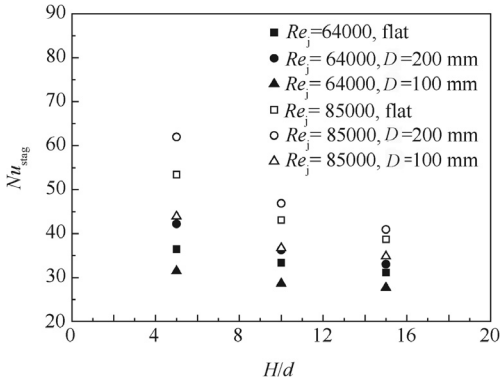

Fig. 8 Nusselt number at stagnation point for varying H/d ($d = 2$ mm).

this attenuation of the jet velocity is completed within a small range near the stagnation point, so the heat transfer is less affected by H/d for a farther distance.

4.4. Curvature effects

Heat transfer distributions affected by curvature along both chordwise and spanwise directions are investigated in this section for jet Reynolds number $Re_j = 27000$–130000, relative nozzle to surface distance $H/d = 3.3$–30, and relative surface curvature $d/D = 0.005$–0.030. The relative surface curvature

Cr was calculated by the ratio of jet diameter d to the surface diameter D, and thus different Cr values could be obtained by varying surface diameter D, as well as the jet diameter d.

4.4.1. Curvature effects on a fixed surface

The average heat transfer performance varying with the change of relative surface curvature at different Reynolds numbers is shown in Fig. 9 for a constant surface diameter of $D = 200$ mm. Because Reynolds number changes remarkably with the diameter of jet under the same inlet pressure condition, to figure out the effect of Cr at similar Reynolds number, more tests for jet diameters of $d = 1.5$ mm and $d = 2.5$ mm were conducted. It can be inferred from the figure that Nu_{avg} increases with the increase of Cr at a given Reynolds number.

It is consistent with the results of many other studies that relative curvature enhances average heat transfer[18] and increases local Nusselt number[15] as a consequence of the growing Taylor-Görtler vortices along the streamwise direction. However, the authors believe that, for the same Reynolds number, the higher Cr caused by a larger jet diameter would lead to a larger flow rate according to Eq. (2). As it is proved by Bu et al.[23] that average heat transfer performance mainly depends on the flow rate, higher Cr brings better average heat transfer in this section. This point can also explain the results of Lee et al.[27] on the influence of jet diameters, in which they found the local Nusselt number increased with the increasing nozzle diameter near the stagnation point region when Reynolds number was constant.

4.4.2. Curvature effects with changed surface diameters

Fig. 10 presents average Nusselt number of curved and flat surfaces at different H/d for $d = 2$ mm and $Re_j = 64000$, 85000. The relative curvature $Cr = 0.01$ for $D = 200$ mm surface and $Cr = 0.02$ for $D = 100$ mm. The result shows that the average heat transfer performance is weaker for the curved plate than for the flat plate, and Nu_{avg} becomes lower with increasing Cr. The data are interesting since it is against the previous results obtained by Gau and Chung[15] and Yang et al.[18] As a new attempt, there is no similar investigation that can be a reference to explain this phenomenon. Unlike most researches in which different Cr is obtained by altering the jet diameter d, the varied Cr in this section is gained by different surface diameters D instead, which is of high importance in the real aircraft wing anti-icing system as the surface curvature of airfoil changes constantly.

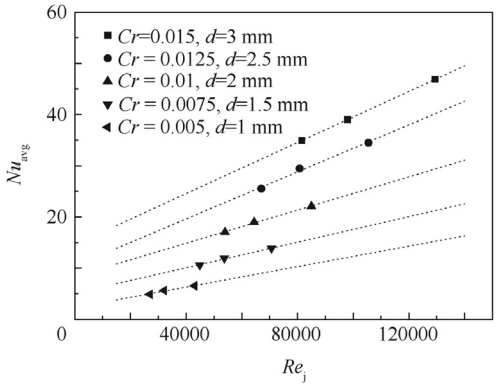

Fig. 9 Average Nusselt numbers for varying Cr on a fixed surface of $D = 200$ mm.

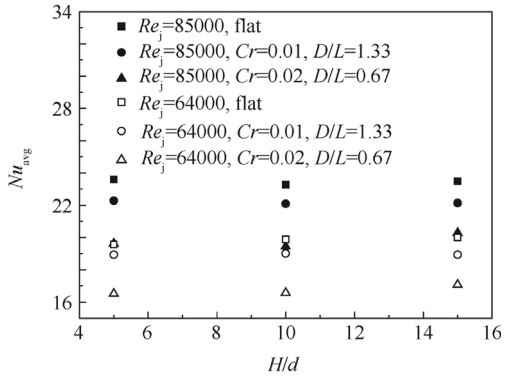

Fig. 10 Average Nusselt number of flat and curved plate for $d = 2$ mm.

An appropriate explanation might be the experiment conducted by Öztekin et al.[25] using dimensionless surface curvature D/L as defined in Section 2 to discuss the curvature effect of a slot jet flow. They found that the average heat transfer performance on the curved plate was stronger than that of the flat plate at $1 \le D/L \le 2.6$. Furthermore, the D/L increased both the local and average Nusselt numbers and the best heat transfer performance was obtained at $D/L = 2.6$. In order to compare the present round jet impingement results with theirs, the average Nusselt numbers are recalculated on the equivalent impinging area (Fig. 11). As the dimensionless surface curvatures D/L in the present work are 0.67 and 1.33, it appears plausible that the different heat transfer performance of the curved plates may be due to the non-reaching of the optimal dimensionless surface curvature D/L to get the best performance.

For a better understanding of the effects on different surfaces, the distributions of local Nusselt number in chordwise s and spanwise y direction near the stagnation region are presented in Fig. 12 for $D/L = 0.67$, 1.33 and flat surface. As shown in Fig. 12, the increase of D/L enhances heat transfer at stagnation point as Nu_{stag} of $D/L = 1.33$ is larger than that of flat surface, while Nu_{stag} of $D/L = 0.67$ is smaller. Another evidence of D/L's effect can be seen from the Nusselt distribution characteristics between s and y direction. When

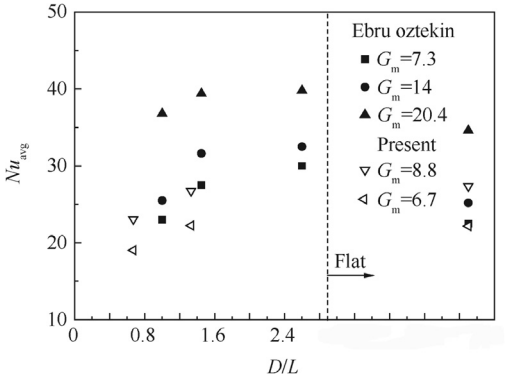

Fig. 11 Effect of D/L on average Nusselt number.

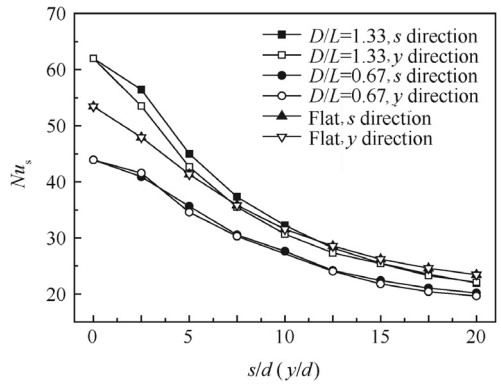

Fig. 12 Nusselt number in s and y direction for Re = 86000, d = 2 mm.

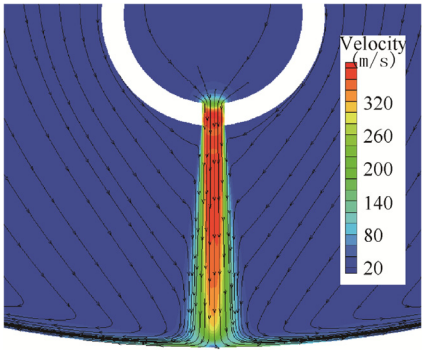

Fig. 13 Streamlines in velocity profile of y = 0 mm.

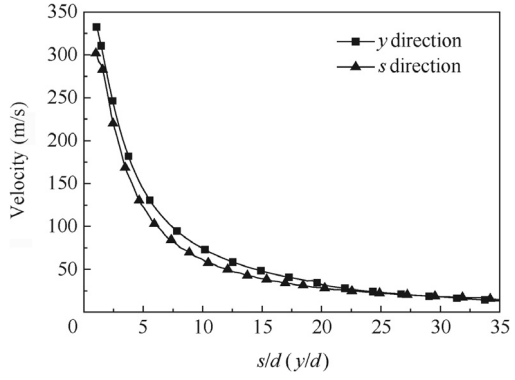

Fig. 14 Velocity distributions along s and y direction.

D/L = 1.33, the local Nusselt number in s direction is slightly higher than that in y direction at the same distance. However, when D/L = 0.67, the local Nusselt numbers are approximately equal in both directions. It is indicated that the curvature effect contributes to thinning the boundary layer and raising turbulent intensity in s direction for a larger D/L, while for a small D/L, the curvature resists the jet flowing along s direction and reduces the heat transfer in this direction, where the local Nusselt number is supposed to be larger than that in y direction due to the thinner boundary layer caused by the curvature.

A numerical simulation method is used to provide the important flow features along different directions. Fig. 13 shows the streamlines in the velocity profile of y = 0, which indicate that the surrounding air is entrained by the jet. The flow velocity of the jet impinging on D = 200 mm surface in the wall jet region is presented in Fig. 14. The air velocity along y direction is higher than that in s direction within a relatively large range near the stagnation point. It is indicated that the curvature confines the flow along chordwise direction, forcing part of the air to flow along the spanwise direction, and therefore reduces the heat transfer.

5. Experimental data-based correlation equations

5.1. Correlation equation for fixed surfaces

To compare with the previous results of other researchers, the correlation equations of Nu_{avg} are given for each concave surface in terms of Re_j, H/d and relative surface curvature d/D:

For D = 100 mm plate,

$$Nu_{avg} = 1.07 Re_j^{0.689} (H/d)^{-0.0035} (d/D)^{1.23} \quad (9)$$

where $27000 \le Re_j \le 130000$, $3.3 \le H/d \le 30$ and $0.01 \le d/D \le 0.03$.

For D = 200 mm plate,

$$Nu_{avg} = 4.44 Re_j^{0.633} (H/d)^{0.0337} (d/D)^{1.22} \quad (10)$$

where $27000 \le Re_j \le 130000$, $3.3 \le H/d \le 30$ and $0.005 \le d/D \le 0.015$.

Nu_{avg} varies according to $(Re_j)^{0.689}$ for D = 100 mm and $(Re_j)^{0.633}$ for D = 200 mm, which approximately agrees with Gau and Chung's[15] result of $(Re_j)^{0.68}$ and Fenot's[24] result of $(Re_j)^{0.72}$. The exponential values of d/D are much larger than those of H/d, suggesting that changing H/d would have much fewer influence on Nu_{avg} than changing d/D.

The calculated results $Nu_{avg,c}$ of Eqs. (9) and (10) compared with the experimental data $Nu_{avg,e}$ are presented in Fig. 15, which show a very good fitting with the experimental data.

5.2. Correlation equation for fixed jet diameter

Based on the experimental results, the correlation equation of the average Nusselt number Nu_{avg} in terms of jet Reynolds

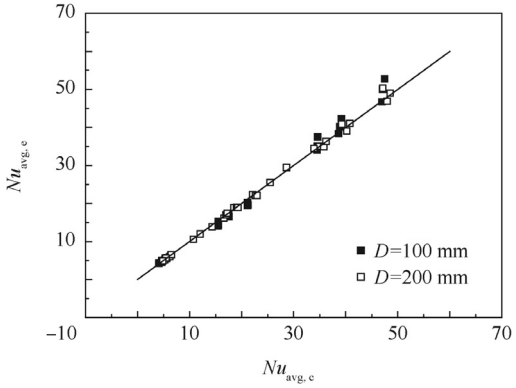

Fig. 15 Comparison between calculated results and experimental data for fixed surfaces.

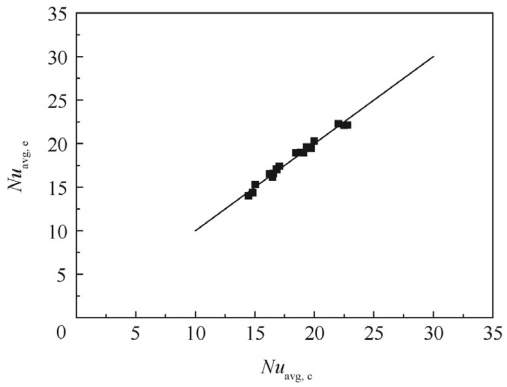

Fig. 16 Comparison between calculated results and experimental data for $d = 2$ mm.

number Re_j, relative nozzle to surface distance H/d, and dimensionless surface curvature D/L for a fixed diameter $d = 2$ mm is obtained as follow:

$$Nu_{avg} = 0.0065 Re_j^{0.638} (H/d)^{0.0312} (d/D)^{-0.183} = 0.014 Re_j^{0.638} (H/d)^{0.0312} (D/L)^{0.183} \quad (11)$$

for $54000 \le Re_j \le 86000$, $5 \le H/d \le 15$ and $0.67 \le D/L \le 1.33$.

The average Nusselt number increases with growing Reynolds number and increasing dimensionless surface curvature D/L (i.e., with decreasing d/D), which agrees with the results of Öztekin et al.[25] The calculated results of Eq. (11) compared with the experimental data are presented in Fig. 16, which are in good agreement with the experimental data.

6. Conclusions

Extensive experimental study of the heat transfer performance of a round jet impingement on concave surfaces under constant heat fluxes were conducted in this work, where the effects of jet Reynolds number Re_j, the relative nozzle to surface distance H/d and the relative surface curvature d/D on local and average Nusselt number were investigated, and experimental data-based correlation Nu_{avg} equations were obtained. The major conclusions of the present study have been summarized as follows:

(1) Both stagnation point and average Nusselt numbers increased significantly with increasing jet Reynolds number, suggesting that increasing the inlet jet pressure or flow rate is an effective way to enhance the heat transfer of an anti-icing system.
(2) The stagnation point Nusselt number increased as the relative nozzle to surface distance decreased in the range of $3.3 \le H/d \le 30$, and the effect of H/d was mainly presented near the stagnation region of $s/d < 12.5$.
(3) Two opposite effects of surface curvature on jet impingement heat transfer performance were observed. For a fixed surface diameter, the relative surface curvature d/D increased both stagnation point and average Nusselt numbers with increasing jet diameter d. In contrast, for a fixed d, the average Nusselt number declined with increasing d/D. The Nu_{avg} increased as the dimensionless surface curvature D/L increased before reaching the maximum value for an optimal D/L.
(4) Under the same jet impingement condition (jet diameter and inlet pressure), the average Nusselt number over the entire surface was influenced more by the confinement effect than by the enhancement effect within the range of the present experiment, leading to a smaller Nu_{avg} for the concave surfaces.
(5) Based on the experimental data, correlation equations of the average Nusselt number were acquired and experimentally validated, which are applicable to the following parameter ranges: $27000 \le Re_j \le 130000$, $3.3 \le H/d \le 30$ and $0.005 \le d/D \le 0.03$.

Further experiments of jet impingement on large surface diameters are planned to identify the optimum d/D for a given d, and to examine the practical anti-icing effect under different curvatures.

Acknowledgements

This work was supported by the National Natural Science Foundation of China (No. 51206008) and the EU Marie Curie Actions-International Incoming Fellowships (No. FP7-PEOPLE-2013-IIF-626576).

References

1. Zhang JZ, Xie H, Yang CF. Numerical study of flow and heat transfer characteristics of impingement/effusion cooling. *Chin J Aeronaut* 2009;**22**(4):343–8.
2. Liu HY, Liu CL, Wu WM. Numerical investigation on the flow structures in a narrow confined channel with staggered jet array arrangement. *Chin J Aeronaut* 2015;**28**(6):1616–28.
3. Gardon R, Cobonpue J. Heat transfer between a flat plate and jets of air impinging on it. International heat transfer conference; 1961. p. 454–60.
4. Goldstein RJ, Behbahani AI, Heppelmann K. Streamwise distribution of the recovery factor and the local heat transfer coefficient to an impinging circular air jet. *Int J Heat Mass Transf* 1986;**29**(8):1227–35.
5. Hrycak P. Heat transfer from round impinging jets to a flat plate. *Int J Heat Transf* 1983;**26**(12):1857–65.
6. Beltaos S. Oblique impingement of circular turbulent jets. *J Hydraulic Res* 1976;**14**(1):17–36.
7. Sparrow EM, Lovell BJ. Heat transfer characteristics of an obliquely impinging circular. *J Heat Transf ASME* 1980;**102**(2):202–9.
8. Goldstein RJ, Timmers JF. Visualization of heat transfer from arrays of impinging jets. *Int J Heat Mass Transf* 1982;**25**(12):1857–68.
9. Goldstein RJ, Franchett ME. Heat transfer from a flat surface to an oblique impinging jet. *J Heat Transf ASME* 1988;**110**(1):84–90.
10. Lytle D, Webb BW. Air jet impingement heat transfer at low nozzle-plate spacings. *Int J Heat Mass Transf* 1994;**37**(12):1687–97.
11. Attalla M, Salem M. Experimental investigation of heat transfer for a jet impinging obliquely on a flat surface. *Exp Heat Transf* 2015;**28**(4):378–91.
12. Metzger DE, Yamashita T, Jenkins CW. Impingement cooling of concave surfaces with lines of circular air jets. *J Eng Power* 1969;**91**(3):149–55.
13. Hrycak P. Heat transfer from a row of impinging jets to concave cylindrical surfaces. *Int J Heat Mass Transf* 1981;**24**(3):407–19.

14. Mayle RE, Blair MF, Kopper FC. Turbulent boundary layer heat transfer on curved surfaces. *J Heat Transf ASME* 1979;**101**(3):521–5.
15. Gau C, Chung CM. Surface curvature effect on slot-air-jet impingement cooling flow and heat transfer process. *J Heat Transf ASME* 1991;**113**(4):858–64.
16. Cornaro C, Fleischer AS, Goldstein RJ. Flow visualization of a round jet impinging on cylindrical surfaces. *Exp Therm Fluid Sci* 1999;**20**(2):66–78.
17. Lee DH, Chung YS, Won SY. The effect of concave surface curvature on heat transfer from a fully developed round impinging jet. *Int J Heat Mass Transf* 1999;**42**(13):2489–97.
18. Yang G, Choi M, Lee JS. An experimental study of slot jet impingement cooling on concave surface: effects of nozzle configuration and curvature. *Int J Heat Mass Transf* 1999;**42**(12):2199–209.
19. Brown JM, Raghunathan S, Watterson JK, Linton AJ, Riordon D. Heat transfer correlation for anti-icing systems. *J Aircraft* 2002;**39**(1):65–70.
20. Papadakis M, Wong SJ, Yeong HW, Wong SC. Icing tunnel experiments with a hot air anti-icing system. Reston: AIAA; 2008. Report No.: AIAA-2008-0444.
21. Papadakis M, Wong SJ, Yeong HW, Wong SC. Icing tests of a wing model with a hot-air ice protection system. Reston: AIAA; 2010. Report No.: AIAA-2010-7833.
22. Imbriale M, Ianiro A, Meola C, Cardone G. Convective heat transfer by a row of jets impinging on a concave surface. *Int J Therm Sci* 2014;**75**(1):153–63.
23. Bu XQ, Peng L, Lin GP, Bai LZ. Experimental study of jet impingement heat transfer on a variable-curvature concave surface in a wing leading edge. *Int J Heat Mass Transf* 2015;**90**(1):92–101.
24. Fenot M, Dorignac E, Vullierme JJ. An experimental study on hot round jets impinging a concave surface. *Int J Heat Fluid Flow* 2008;**29**(4):945–56.
25. Öztekin E, Aydin O, Avcı M. Heat transfer in a turbulent slot jet flow impinging on concave surfaces. *Int Commun Heat Mass Transf* 2013;**44**(5):77–82.
26. Martin EL, Wright LM, Crites DC. Impingement heat transfer enhancement on a cylindrical, leading edge model with varying jet temperatures. *J Turbomach* 2012;**135**(3):323–34.
27. Lee DH, Song J, Jo MC. The effects of nozzle diameter on impinging jet heat transfer and fluid flow. *J Heat Transf* 2004;**126**(4):554–7.